Polym. Korea, Vol. 48, No. 4, pp. 403-412 (2024)
https://doi.org/10.7317/pk.2024.48.4.403

ISSN 0379-153X(Print)
ISSN 2234-8077(Online)

MXene/rGO 필러를 사용한 에폭시 복합체의 전자기파 차폐 성능에 미치는 rGO의 영향

이승욱 · 강지수 · 김무진 · 윤근병†

경북대학교 고분자공학과

(2024년 3월 12일 접수, 2024년 4월 27일 수정, 2024년 4월 27일 채택)

The Effect of rGO on the Electromagnetic Interference Shielding Performance of Epoxy Composites Incorporating MXene/rGO Fillers

Seong Wook Lee, Ji-Soo Kang, Mu Jin Kim, and Keun-Byoung Yoon†

Department of Polymer Science and Engineering, Kyongpook National University, Daegu 41566, Korea

(Received March 12, 2024; Revised April 27, 2024; Accepted April 27, 2024)

초록: 3D 구조의 탄소물질은 전자기파 차폐 성능을 향상시키며, 3D 상호 전도성 네트워크는 기공을 풍부하게 하여 광대역 마이크로파 흡수 및 전자기파 차폐를 위한 효과적인 임피던스 매칭을 위한 다양한 인터페이스가 생성된다. 이러한 계층적 구조는 넓은 표면적과 풍부한 인터페이스를 가져서 전자기파 에너지 흡수를 촉진하여 전자기파 차폐 성능을 향상시킬 수 있다. 파우더, 일축방향성 3D 타입 및 폼 타입의 필러는 MXene과 rGO를 혼합하여 제조하였으며, 이 필러를 에폭시에 함침시켜 복합체를 제조하고 에폭시 복합체의 전자가파 차폐 성능을 평가하였다. 15 wt% 폼 타입 필러를 함유한 에폭시 복합체의 electromagnetic interference shielding efficiency(EMI SE)는 18 GHz에서 90 dB 이상을 나타내었으며, MXene에 rGO를 첨가함으로써 광대역에 걸쳐 에폭시 복합체의 electromagnetic interference shielding efficiency(EMI SE)가 증가하는 상승 효과를 나타내었다. 폼 타입 MXene/rGO 필러는 우수한 electromagnetic interference shielding efficiency(EMI SE) 값을 나타내어, 전자기파 차폐를 위한 고분자 복합체에 유용한 재료로 판단된다.

Abstract: The 3D structure of carbon materials enhances electromagnetic (EM) wave shielding performance, while the 3D interconnective network improves porosity to create various interfaces for effective impedance matching for broadband microwave absorption and electromagnetic interference (EMI) shielding. This hierarchical structure feature, with its large specific surface area and abundant interfaces, can promote EM energy absorption, thereby enhancing EM shielding performance. The powder-, unidirectional-, and foam-type fillers were prepared by mixing MXene and rGO, and these fillers were impregnated into epoxy to produce composites, evaluating the EM wave shielding performance of the epoxy composites. The EMI shielding effectiveness (EMI SE) value of epoxy composites containing 15 wt% foam-type filler exhibited over 90 dB at 18 GHz, and the addition of rGO to MXene showed an increasing effect on the EMI SE of the epoxy composite across a broadband. The foam-type MXene/rGO filler demonstrated excellent EMI SE values, making it a valuable material for polymer composites for EM wave shielding purposes.

Keywords: electromagnetic wave shielding, foam-type MXene/rGO, 3D structure, epoxy composites.

Introduction

With the development of highly integrated electronic devices in response to the needs of modern telecommunications and information technologies, the issue of electromagnetic interference (EMI) affecting electronic devices and human health has become a major topic of interest. Moreover, radar and advanced military detection technologies pose a serious threat to aircraft and weapons. Therefore, the demand for new microwave absorbers and electromagnetic (EM) shielding materials has attracted tremendous attention.[1-3]

EM wave shielding by reflection mainly corresponds to metal-based materials. However, most of the studies have been conducted on materials with high absorption, such as carbon-based materials. Extensive research is focused on the development of high-performance EM absorption materials with lightweight,

#These authors equally contributed to this work.
†To whom correspondence should be addressed.
kbyoon@knu.ac.kr, ORCID 0000-0001-5174-8236

broadband frequency, and excellent absorption properties, including carbon fiber,[4] graphene,[5] carbon nanotubes[6] and MXene.[7] These carbon -based nanomaterials have attracted great interest in emerging engineering fields such as EMI shielding, electronics, and energy storage owing to their excellent electrical conductivity, high specific surface area, and exceptional chemical stability.[8]

The process of exfoliation process is closely related to the dispersion of 2D materials in a colloidal state, including graphene, hexagonal boron nitride, clay, and layered double hydroxide. These materials are exfoliated and stabilized in colloidal solutions with surfactants, utilizing surface charges for stabilization. However, their dispersion in aqueous solutions is not efficient.[9,10] In contrast, MXene exhibits excellent dispersion and stability in aqueous solutions and polar solvents, including dimethylformamide, *N*-methyl-2-pyrrolidone, dimethyl sulfoxide, and propylene carbonate.[11] Furthermore, MXene is more manageable than other 2D materials owing to the cost and safety advantages associated with exfoliation in an aqueous environment. As a result, it finds diverse applications across various fields. The EMI shielding efficiency (SE) of an MXene film (45 μm thickness) has been reported to be 92 dB.[12] Sun *et al*.[13] reported high electrical conductivity (1081 S/m) and EMI SE (54 dB) by mixing polystyrene with an MXene dispersion solution through electrostatic self-assembly. Liu *et al*.[14] reported a lightweight, hydrophobic, and durable MXene foam with an EMI SE of 70 dB fabricated using hydrazine hydrates, which promoted multiple attenuations of EM waves.

MXene is a promising material for EM pollution control, as it has unique metallic properties with a large surface area and excellent electrical conductivity in a typical 2D layered structure.[12,15] The excellent EMI shielding performance of MXene can effectively attenuate EM waves introduced inside the material due to its favorable electron coupling between layers and excellent electrical conductivity (4600 S/cm).

Among carbon-based materials, graphene is well known to have excellent microwave absorption. It has been considered an important material for obtaining excellent EM absorption performance owing to its low density, large surface area, strong charge-carrier mobility, and high dielectric loss.[8] Graphene oxide (GO) is more reactive than graphene because it contains oxygen-functional groups such as carboxyl, epoxy, and hydroxyl groups.[16] Reduced graphene oxide (rGO) is a preferred alternative to GO as it has high conductivity resulting from the reduction of oxygen groups. Thus, it is suitable for applications that require better electrical properties.[17] The applicability of rGO for EMI shielding has been widely studied for EMI shielding owing to its dipole and orientation polarization originating from its abundant defects and hydroxyl groups, which improve its absorption performance.[18]

Liang *et al*. reported that EMI SE showed 21 dB in the X-band when 15 wt% was added to the epoxy composite using solution-processable functionalized rGO.[19] The free-standing rGO film was produced by thermal reduction of GO film, and its EMI shielding performance was 61 dB at 12.4 GHz.[20]

GO aerogels with 3D structures have been proven to be efficient EMI shielding materials with superior advantages of low density, strong absorption of microwaves, and multi-band applicability. More importantly, most GO aerogels and their composites exhibit absorption-dominated shielding performance, which is exactly the future developing trend for EMI shielding materials.[21] Shen *et al*. reported the foaming of layered graphene films into porous graphene foams could improve their performance for absorbents.[22]

Furthermore, building a heterostructure architecture by mixing two or more different materials is a practical strategy to achieve the synergistic effect in many ways. Recently, MXene/graphene heterostructures have exhibited several applications, including metal ion batteries,[23] supercapacitors,[24] sensors,[25] and EMI shielding.[26] Liu *et al*. prepared an MXene/rGO composite film by directly mixing MXene and GO after vacuum filtration and chemical reduction, which afforded an efficient EMI SE of 50.2 dB.[27] In another study, Zhang et al. produced a sandwich structure by loading rGO/MXene on a nonwoven fabric through an immersion-drying-reduction method, where the shielding performance increased owing to the increase in MXene content and reached a high EMI SE of ~60 dB.[28]

Current studies have concentrated on 3D porous aerogel materials as fillers for EMI shielding. Aerogels are considered promising as lightweight and high-performance EMI shielding materials because of their microporosity, high electrical conductivity, and high specific surface area characteristics. Unfortunately, it is difficult to construct MXene as a 3D assembly owing to its intrinsic weak gelation capability, which limits its application in lightweight EMI shielding materials. Although using MXene itself to create 3D structures is difficult, it is possible to fabricate 3D structures with graphene by introducing GO. Zhao *et al*. developed a highly conductive 3D porous aerogel by mixing MXene and GO suspension and subjecting it to hydrothermal treatment, followed by freeze-drying.[29] Song *et al*.[30] reported that 3D rGO-MXene fully exhibited the synergy effect between rGO and MXene, and significantly improved

the electrical conductivity and EMI SE of rGO-MXene/epoxy composites. Most of the existing research is concerned with the self-EM absorption properties of rGO-MXene, while few studies have been reported on the absorption of EM waves in polymer composites using them. Polymer composite materials have the advantages of high strength, low density, and easy processing, and many studies are being conducted on combining microwave-absorbing materials with carbon-based nanomaterials.[31,32]

In this research, MXene was employed as an electromagnetic interference shielding material due to its superior dispersibility in an aqueous solution. However, the standalone use of MXene resulted in suboptimal electromagnetic interference shielding performance. To enhance this property, rGO, recognized for its exceptional shielding capabilities, was incorporated into MXene to produce fillers. The electromagnetic interference shielding properties of the epoxy composites were then evaluated based on different rGO concentrations.

To assess the synergy effect of EMI shielding by incorporating rGO into MXene, two types of fillers were prepared: a powdered physically mixed MXene/rGO filler and a porous directional 3D MXene/rGO filler (Scheme 1).

The EMI shielding properties of epoxy composites were then evaluated. Furthermore, MXene/rGO foam was prepared by mixing MXene, known for its excellent dispersity in aqueous solutions, with rGO, renowned for its exceptional electrical conductivity and EM wave shielding properties. To prepare a composite capable of preserving the internal structure of the MXene/rGO foam, we employed epoxy with a suitably low viscosity as the polymer matrix and examined the EMI shielding performance of the impregnated composites. The EMI SE of the epoxy composites was evaluated with consideration given to the types of filler, filler content, and rGO content.

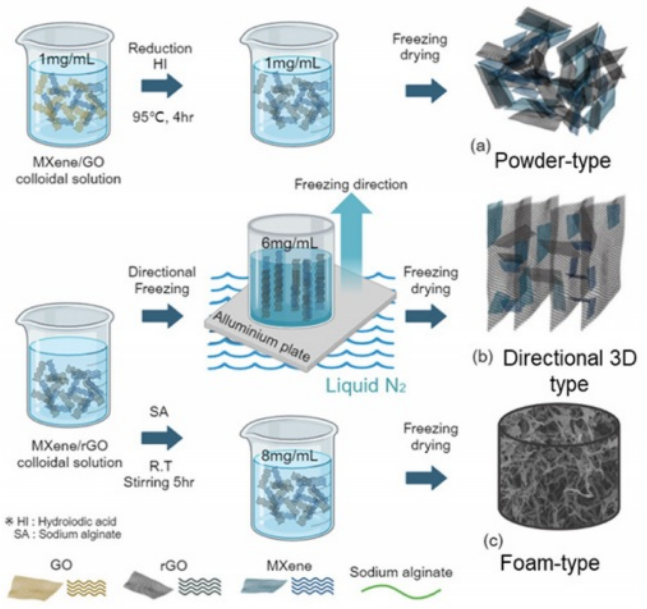

Scheme 1. Preparation of MXene/rGO fillers: (a) powder-; (b) directional 3D-; (c) foam-type.

Experimental

Materials. Expanded graphite (EG, Timcal Graphite Carbon, Switzerland, ~100 μm, ≥99.9%), titanium aluminum carbide (MAX(Ti_3AlC_2), 11 Technology Co., China, ~38 μm, ≥98%), lithium fluoride (LiF, Alfa Aesar, USA, >99%), potassium permanganate ($KMnO_4$, 99%, Sigma Aldrich, US), hydrogen iodide (HI, Daejung Chemicals and Metals Co., ≥57%), sodium alginate (SA, $(C_6H_7NaO_6)_n$, Duksan Chemical co.)), and commercial-grade epoxy (EpoxAcast 690, Smooth-on, Inc., USA) were used without further purification.

Synthesis of MXene Colloidal Solution. MXene was synthesized by selectively etching the Al layer of MAX (Ti_3AlC_2) with LiF and HCl[33] as follows. 3 g of LiF and 30 mL of HCl were added in a 50 mL Teflon beaker and stirred for 30 minutes, and then 3 g of MAX powder was added to the beaker very slowly and reacted at room temperature for 24 h. After the reaction, the mixture was repeatedly washed with distilled water through centrifugation. The washed mixture was sonicated for 30 minutes to exfoliate the MXene layers, and the sonicated mixtures were centrifuged to collect the supernatants, which contained exfoliated MXene.

Preparation of Powder-type MXene/rGO Fillers. Graphene oxide (GO) was prepared by oxidizing graphite flakes according to the modified Hummers method.[34] The obtained GO and MXene were dispersed in DMSO (1 mg/mL) and sonicated to obtain a uniform colloidal solution. The mixed MXene/GO filler was reduced with HI.[35] The powder-type MXene/rGO fillers were prepared by freeze-drying colloidal solutions at -80 ℃ for 48 h. The mixtures of MXene and GO at weight ratios of 8/2, 5/5, and 2/8 were denoted as MGP82, MGP55, and MGP28, respectively.

Preparation of Directional 3D-type MXene/rGO Fillers. The directional freezing method assembles dispersed MXene/rGO mixtures into a vertically oriented porous network using anisotropically grown ice crystals as a template (Scheme 1). To prepare the directional 3D-type MXene/rGO filler, a colloidal solution (6 mg/mL in DMSO) was poured into a plastic tube

equipped with an aluminum bottom and placed over liquid nitrogen, allowing unidirectional freezing from bottom to top, followed by freeze-drying. The resulting directional 3D-type MXene/rGO fillers, which mixed MXene and GO at weight ratios of 8/2, 5/5, and 2/8, were denoted as MGD82, MGD55, and MGD28, respectively.

Preparation of 3D Foam-type MXene/rGO Fillers. The MXene/rGO colloidal solution (8 mg/mL) was prepared at the same mass ratios as powder and directional 3D-types. Sodium alginate was added to MXene/rGO colloidal solution (filler/SA = 2/1, 1/1, 1/2, 1/4; wt/wt), stirred for 5 h, and then freeze-dried to prepare the foam-type MXene/rGO filler.[36] Additionally, MXene/rGO dispersion (4, 8, 12, 16 mg/mL) was used to investigate the effect on the internal structure of the foam according to the filler concentration, with the weight ratio of MXene/rGO filler and SA fixed at 1/1.

Preparation of MXene-rGO/epoxy Composite. The epoxy composite was prepared by filling a specimen mold with various types of fillers, slowly adding epoxy, and thermally curing it under constant pressure at 80 ℃ for 6 h. Recognizing the thickness of the specimen as a crucial factor influencing the EMI SE, the specimens used for EMI SE measurements in this experiment were fabricated to a thickness of 1.5 mm.[37]

Characterization. The morphology of the fillers and epoxy composites was examined using scanning electron microscopy (SEM; SU8230, Hitachi, Japan).

The EMI shielding effect of composites was obtained by measuring electromagnetic parameters in the frequency range of C-band, X-band, and Ku-band (0.5-18.0 GHz) using a vector network analyzer (NA, E8364B, Agilent, USA).

Results and Discussion

Morphologies of MXene/rGO Filler. Figure 1 shows the morphology of the powder-type and directional 3D-type MXene/rGO filler as a function of the rGO content.

The powder-type MXene nanosheets exhibit fully exfoliated into a few layers, whereas rGO does not show individual sheets, the sheets are agglomerated and exhibit some wrinkling. In its GO state before reduction, GO exists as a few layers due to effective exfoliation. However, during the reduction process, agglomeration occurs, accompanied by wrinkling.[38] This agglomeration and wrinkling phenomena intensify with higher GO content, attributed to the insertion of MXene between GO sheets, which helps suppress sheet wrinkling and stacking. Nevertheless, if the GO content surpasses the MXene content, the stacking of

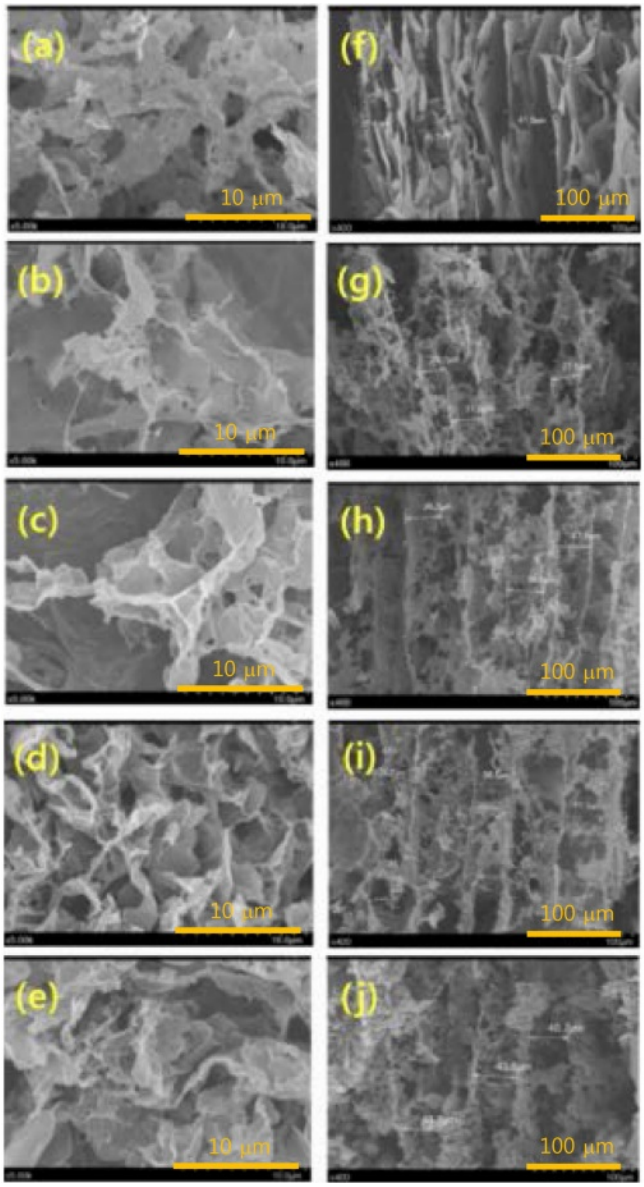

Figure 1. SEM images of the powder- and directional 3D-types of MXene, MXene/rGO filler, and rGO: (a) MXene powder; (b) MGP82; (c) MGP55; (d) MGP28; (e) rGO; (f) MXene directional 3D-type; (g) MGD82; (h) MGD55; (i) MGD28; (j) rGO diresctional 3D-type.

rGO becomes more predominant during the reduction process. Even when GO was introduced into MXene, powder-type MXene/rGO fillers randomly stuck to each other without forming a specific architecture.

It is known that when 2D nanomaterial colloids are fabricated using a unidirectional freezing method, channels are formed in which nanomaterials aligned in the direction of ice crystal growth. Accordingly, MXene/rGO colloids were also produced using the unidirectional freezing method, and the

internal structures are shown in Figure 1.

The directional 3D-type MXene exhibits a continuous and relatively dense 3D network coupled with a thin lamellar structure, and the cell surface has a relatively smooth appearance. Even in the case of MXene/rGO fillers, MXene maintains a 3D network combined with a continuous cell structure, however. the cell surface is rough and rGO appears wrinkled and entangled.

The cell size became irregular, and large cells were formed with an increase in the rGO content. As the rGO content increased, the average channel width between the parallel cells slightly increased from ~36 μm in MGD82 to ~40 μm in MGD28. This expension is attributed to the growth of larger ice crystals around rGO, which has a large surface area and is hydrophilic. The MXene/rGO filler formed a uniform and overall aligned cellular structure through the unidirectional assembly of rGO and MXene sheets. Similar regular cellular structures were observed for fillers with different ratios of MXene/rGO components. Although the exact reason for the variation in channel width is not clear, the nucleation of ice crystals is considered crucial in determining the cell structure, influenced by various parameters such as the concentration and cooling rate of the suspension.[26,39]

rGO aerogel is a lightweight 3D material composed of rGO flakes with highly interconnected porous structures. The processing of rGO aerogel is influenced by various factors, including concentrations, filler size, temperature, type of reducing agent, and methods of water removal from the aerogels.[40,41] Despite the challenges of creating an aerogel using MXene alone, MXene/rGO foam with a porous structure was prepared by incorporating GO, which makes it easy to form an aerogel.

To examine the effect of MXene/rGO colloid concentration on the internal microstructure of foam, a foam was prepared using colloid concentrations ranging from 4 to 16 mg/mL, and a filler/SA weight ratio set at 1/1.

Figure 2 shows that the pore structure of the foam became much finer as the concentration increased from 4 to 12 mg/mL. The foam-type filler, prepared using the MXene/rGO colloidal dispersion at high concentrations, exhibited a denser network with a 3D porous structure. Notably, the foam produced with an MXene/rGO filler concentration of 4 mg/mL did not properly form macropores. Furthermore, the foam prepared with the highest concentration of 16 mg/mL exhibited small pores, but most of the fillers overlapped, resulting in low porosity and dense foam.

Continuous porous structures were achieved with filler concentrations between 8 and 12 mg/mL. However, obtaining a porous foam became virtually impossible when the filler concentration exceeded 12 mg/mL, highlighting the crucial role of filler concentration in MXene/rGO foam formation.

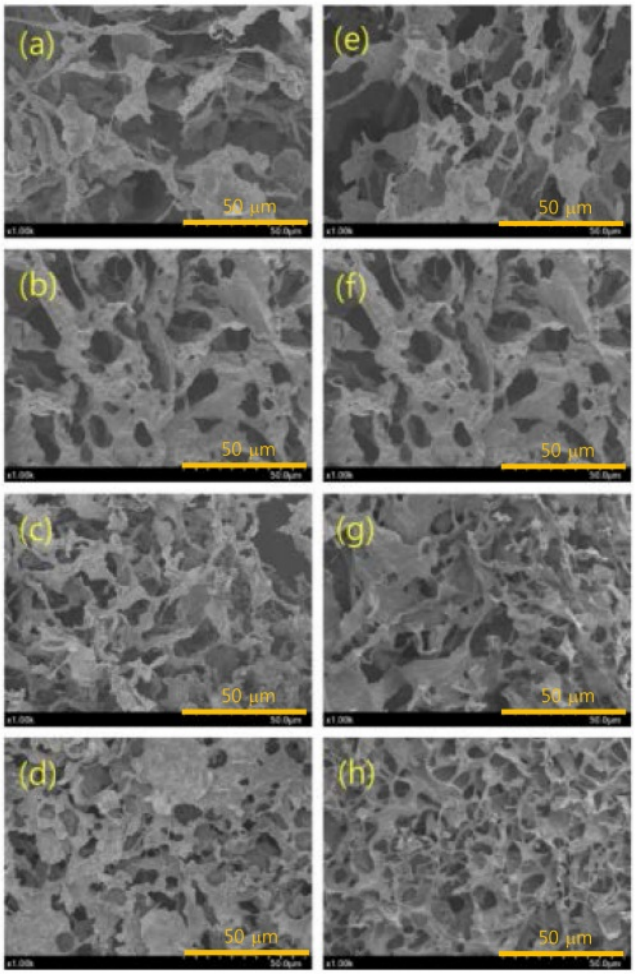

Figure 2. SEM images corresponding to the filler and surfactant concentrations in foam-type fillers prepared with MXene/rGO at a 1/1 weight ratio. Filler concentrations are as follows: (a) 4 mg/mL; (b) 8 mg/mL; (c) 12 mg/mL; (d) 16 mg/mL. The weight ratios of fillers to surfactants are represented as (e) 2/1; (f) 1/1; (g) 1/2; (h) 1/4.

These findings are supported by the apparent density when an increase in MXene/rGO filler concentration led to a rise in the apparent density of the foam to 0.012, 0.028, 0.042, and 0.055 g/cm^3.

The concentrations of rGO and surfactants are known to influence the structure and pore size of rGO aerogel.[42,43] Accordingly, the effect of SA concentration on the porous structure of the foam with an MXene/rGO concentration of 8 mg/mL was investigated, and the corresponding SEM images are shown in Figure 2.

As the SA concentration increased, the spacing between the fillers decreased, leading to a reduction in the average pore size. This phenomenon could be attributed to the accelerated gelation process facilitated by adding SA, which induces interactions between the rGO layers and the formation of folded rGO sheets through reduction.

The MXene/rGO foam, prepared with the filler/SA weight ratio of 1/1, exhibited continuous pores. However, an increased amount of SA enhanced filler interactions, causing overlap and resulting in non-continuous pores. The reduction of MXene/rGO foam by the reduction of GO led to shape change or microcorrugations, such as bending of the rGO sheets. The morphology of the rGO sheet in MXene/rGO foam depended on the SA concentration, remaining flat at low concentrations but folding or bending at higher concentrations. These results also confirmed a sharp increase in the apparent density of MXene/rGO foam to 0.022, 0.028, 0.038, and 0.051 g/cm^3 as the SA content increased.

Based on the above results, the most efficient concentration of MXene /rGO dispersion and the SA ratio were determined. Foam-type MXene/rGO filler was prepared using colloids produced with MXene/rGO weight ratios of 8/2, 5/5, and 2/8 under a concentration of 8 mg/mL, with a filler/SA weight ratio of 1/1, which was the condition for the forming the microporous structure. The internal microstructure of the foam-type MXene/rGO fillers prepared under the mentioned conditions was observed with SEM, and the corresponding images are shown in Figure 3.

The foam-type MXene/rGO fillers exhibit a microporous structure rather than a honeycomb structure, although the macropores are not explicitly observed. The internal structure of the MXene/rGO foam takes shape with loosely arranged nanosheets of randomly oriented rGO, forming macropores between them. The rGO nanosheets adopt a folded structure, continuously interconnected through self-assembly to form a 3D porous network that provides support during freeze-drying, maintaining the foam's shape.[44] SA is attached to the surface of MXene/rGO sheets, acting as an obstruction to prevent sheet recombination and serving as a supportive framework to enhance pores within the foam structure. In other words, SA contributes to the structural stability of the internal architecture during foam formation.[45]

The foam-type MXene/rGO filler exhibited improved macropore formation with increasing rGO content. This enhancement can be attributed to the presence of loosely connected dynamic GO networks in the original dispersion of the GO sheets, resulting from the force balance between electrostatic repulsion and bonding interactions (hydrogen bonds, π-π stacking, hydrophobic effects, etc.).[43,45] Consequently, due to the role of rGO, the internal porosity of the foam-type MXene/rGO filler increased significantly as the rGO content increased.

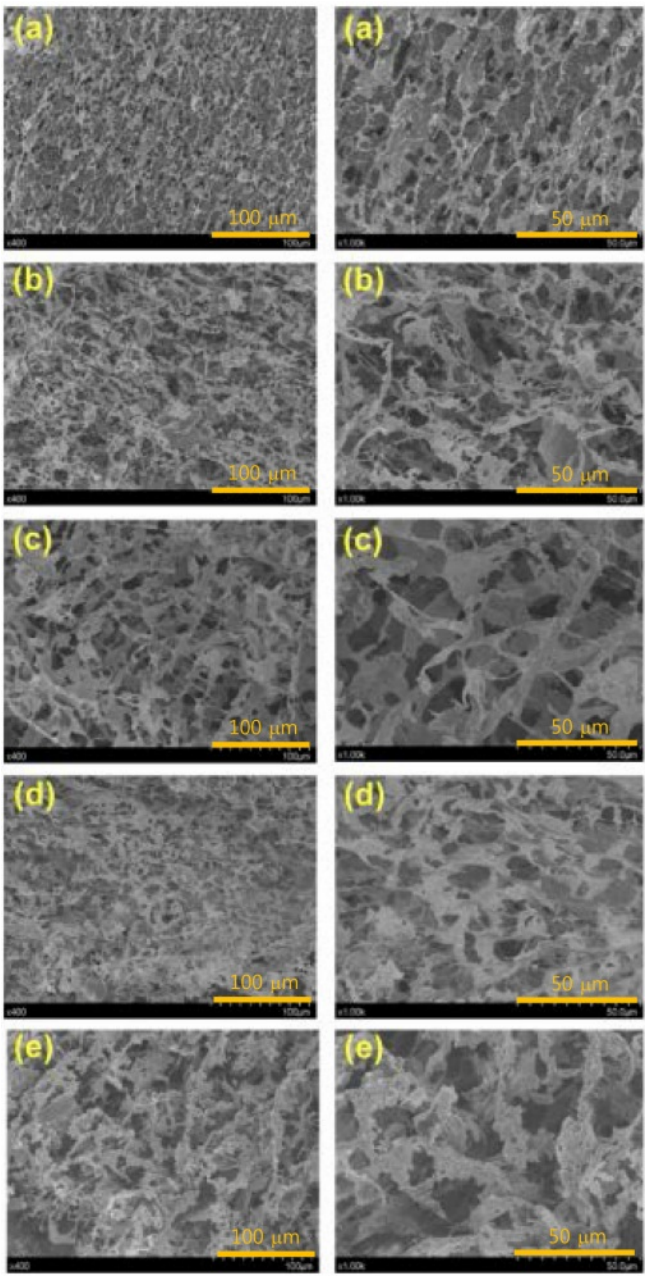

Figure 3. SEM images of the foam type of MXene, MXene/rGO fillers, and rGO: (a) MXene; (b) MGF82; (c) MGF55; (d) MGF28; (e) rGO.

Electromagnetic Interference Shielding Efficiency (EMI SE) of Epoxy Composites. To enhance the effective absorption bandwidth of microwave-absorbent materials, considerations should encompass the chemical structure of filler, morphological control, and the effect of macroscopic control.[46]

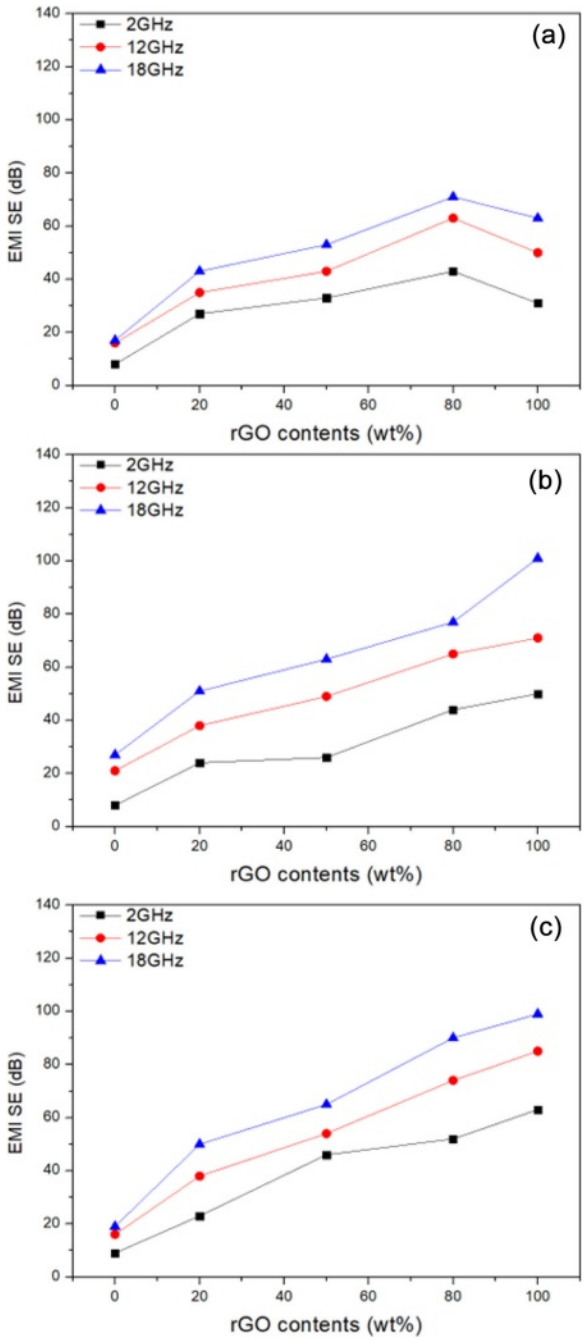

Figure 4. EMI SE graphs of the epoxy composites using MXene/rGO filler according to the filler type and the rGO content of fillers at broadband frequency. Filler contents; 15 wt%: (a) powder-type; (b) directional 3D-type; (c) foam-type.

The EMI performance was investigated according to the filler content of powder-, directional 3D- and foam-type MXene/rGO fillers as well as the weight ratio of MXene and rGO, the corresponding results are shown in Figure 4.

The apparent density of the filler exhibited a notable increase from 0.012 to 0.055 g/cm^3 with an increase in the concentration of the filler dispersion. The filler demonstrated a softer consistency at concentrations below 8 mg/mL, while a rise in concentration led to a reduction in pore size and a transition to a harder state. Consequently, to measure the EMI of the epoxy composite in this study, a fixed concentration of 8 mg/mL was employed for the filler dispersion.

As revealed by Figure 4, the EMI SE of epoxy composites containing 15 wt% of all types MXene/rGO filler increased with the rGO content in the filler increased. Notably, the EMI SE values of the composites using the filler with an rGO content of 20 wt% increased by approximately 4 times, surpassing the EMI performance of the composite using MXene alone.

The epoxy composites with a low powder-type filler content exhibited a synergistic effect upon the introduction of rGO into MXene. SEM images of the powder-type MXene/rGO filler with a low rGO content, shown in Figure 1, indicate that this synergistic effect caused the formation of a network, increasing the surface area by preventing wrinkling of rGO while MXene attached to the rGO surface or connected between sheets owing to the introduction of rGO. In contrast, when using epoxy with 20 wt% powder-type MXene/rGO fillers, the EMI SE value was remarkably high, reaching 118 dB at 18 GHz. However, there was no synergy observed between MXene and rGO, and the EMI SE of the composite increased as the rGO content of the filler increased. In Figure 1(a), a decrease in EMI SE value across the entire frequency range was observed when using only rGO. This reduction is attributed to the larger volume of powder-type rGO fillers compared to MXene/rGO fillers, necessitating the application of pressure during specimen preparation for manufacturing, which makes it difficult to maintain a porous structure.

In the directional 3D-type and foam-type fillers, the EMI SE values of the composites increased with the increasing rGO content in the filler. Although this increase exhibited linearity, a synergistic effect was observed when 20 wt% of rGO was added to MXene. Even at 2 GHz (S-band), the EMI SE value exceeded 20 dB, making it suitable for application in the telecommunication field. However, despite the absence of the synergy effect, the EM wave shielding performance in the Ku-band region surpassed 77 dB as the filler content increased in the composite containing the directional 3D-type and foam-type fillers with a porous structure.

Meanwhile, the electromagnetic shielding of polymer composites using the same filler is more significantly influenced by the filler content compared to the internal structure of the filler.[40]

Therefore, the EMI SE of the epoxy composites was measured according to the contents of the three types of MXene/rGO fillers, as shown in Figure 4. The EMI SE values in the S-, X-, and Ku-band are summarized in Table 1-3 according to the weight ratio of MXene and rGO in the filler and filler content in epoxy composites using powder-type, directional 3D-type, and foam-type MXene/rGO fillers.

The EMI SE value of the composites was evaluated based on the filler content and rGO content in the filler at 2, 12, and 18 GHz, revealing that the EMI SE increases as the filler content increases, irrespective of the frequency band and filler type. In the case of the powder type, the EMI SE value remained around 40~60 dB, regardless of the rGO content, showing no significant change with increasing filler content. However, epoxy composites containing directional 3D-type and foam-type fillers exhibited an increase in EMI SE as the filler content increased, demonstrating excellent electromagnetic wave shielding performance of 78 dB at 12 GHz and approximately 89 dB at 18 GHz.

When comparing the EMI SE values of the epoxy composites, the foam-type filler showed the highest EMI SE value at an MXene/rGO filler content of 15 wt%. However, the directional 3D-type filler had the highest EMI SE value when the filler content was 20 wt%.

Generally, the EMI SE values of carbon materials tend to increase when they form a porous conductive network with 3D structures.[47,48] In 3D graphene with interconnected structures, electrical conduction occurs along the graphene sheets, merging at their junctions and then continuing to adjacent graphene sheets, creating continuous electrical transport paths. The 3D interpenetrating conductive network enriches and improves the pore size, resulting in numerous graphene interfaces that contribute to excellent impedance matching for broadband microwave absorption and EMI shielding.[48] Multiple reflections within the foam pores, *i.e.*, in gaps between the walls of these pores, increased the EMI SE value.

Table 1. EMI SE Values in S-, X-, and Ku-band According to Filler Content and MXene/rGO Weight Ratio of Epoxy Composites Using Powder-type MXene/rGO Fillers

Mxene/rGO weight ratios	Filler contents (wt%)	EMI SE (dB)		
		S-band	X-band	Ku-band
10/0	10	5	10	12
	15	8	16	17
	20	17	26	24
8/2	10	22	32	40
	15	27	35	43
	20	28	38	43
5/5	10	28	37	43
	15	33	43	53
	20	45	57	65
2/8	10	30	40	47
	15	43	63	71
	20	55	95	118
0/10	10	24	30	44
	15	31	50	63
	20	62	103	117

Table 2. EMI SE Values in S-, X-, and Ku-band According to Filler Content and MXene/rGO Weight Ratio of Epoxy Composites Using Directional 3D-type MXene/rGO Fillers

Mxene/rGO weight ratios	Filler contents (wt%)	EMI SE (dB)		
		S-band	X-band	Ku-band
10/0	10	6	15	21
	15	8	21	27
	20	9	22	30
8/2	10	11	22	28
	15	24	38	51
	20	31	44	59
5/5	10	25	36	45
	15	26	49	63
	20	32	55	82
2/8	10	40	48	54
	15	44	65	77
	20	53	78	89
0/10	10	38	42	47
	15	50	71	101
	20	60	97	132

Table 3. EMI SE Values in S-, X-, and Ku-band According to Filler Content and MXene/rGO Weight Ratio of Epoxy Composites Using Foam-type MXene/rGO Fillers

Mxene/rGO weight ratios	Filler contents (wt%)	EMI SE (dB)		
		S-band	X-band	Ku-band
10/0	10	8	12	17
	15	9	16	19
	20	14	20	34
8/2	10	11	22	28
	15	23	38	50
	20	31	44	58
5/5	10	25	36	45
	15	46	54	65
	20	51	66	78
2/8	10	45	54	61
	15	52	74	90
	20	61	91	95
0/10	10	43	62	72
	15	63	85	99
	20	71	98	108

Conclusions

A hierarchical structure was introduced by mixing MXene and rGO to prepare directional 3D-type and foam-type fillers. The EM wave shielding performance was investigated by fabricating epoxy composites using these fillers, and a powder-type MXene/rGO filler was also prepared, evaluated, and compared. The internal structure of the fillers was observed with SEM, revealing that the directional 3D-type and foam-type fillers possessed a microporous structure. The EM wave shielding performance of epoxy composites containing these fillers surpassed that of the powder-type filler, which lacked a porous internal structure. Irrespective of the filler type, the EM wave shielding performance of epoxy composites containing 10 to 15 wt% fillers increased significantly with the addition of rGO, exceeding three times that of MXene alone. Notably, the EMI SE value of epoxy composites containing 15 wt% of foam-type filler reached 90 dB at 18 GHz. The addition of rGO to MXene demonstrated a synergistic effect, increasing the EMI SE of the epoxy composites across broadband frequencies (0.5 ~18 GHz).

Polymer composites utilizing carbon-based shielding materials are recognized as major factors influencing EM wave shielding, considering filler content and internal structure. In epoxy composites, the EMI SE values increased with the MXene/rGO filler content and the rGO content in the filler, further enhanced by the porous internal structure of the filler. The outstanding EMI SE results of foam-type MXene/rGO fillers highlight their potential for use in polymer composites for electromagnetic wave shielding.

Acknowledgment. This research was supported by Kyungpook National University Research Fund, 2022.

Conflict of Interest. The authors declare that there is no conflict of interest.

References

1. Liang, C.; Hamidinejad, M.; Ma, L.; Wang, Z.; Park, C. B. Lightweight and Flexible Graphene/SiC-nanowires/Poly(vinylidene fluoride) Composites for Electromagnetic Interference Shielding and Thermal Management. *Carbon* **2020**, 156, 58-66.
2. Xing, D.; Lu, L.; Xie, Y.; Tang, Y.; Teh, K. S. Highly Flexible and Ultra-thin Carbon-fabric/Ag /Waterborne Polyurethane Film for Ultra-efficient EMI Shielding. *Mater. Des*. **2020**, 185, 108227.
3. Li, Y.; Liu, J.; Wang, S.; Zhang, L.; Shen, B. Self-templating Graphene Network Composites by Flame Carbonization for Excellent Electromagnetic Interference Shielding. *Compos. Pt. B-Eng*. **2020**, 182, 107615.
4. Munalli, D.; Dimitrakis, G.; Chronopoulos, D.; Greedy, S.; Long, A. Electromagnetic Shielding Effectiveness of Carbon Fibre Reinforced Composites. *Compos. Pt. B-Eng*. **2019**, 173, 106906.
5. Shen, B.; Zhai, W.; Zheng, W. Ultrathin Flexible Graphene Film: An Excellent Thermal Conducting Material with Efficient EMI Shielding. *Adv. Funct. Mater*. **2014**, 24, 4542-4548.
6. Qian, K.; Wu, H.; Fang, J.; Yang, Y.; Miao, M.; Cao, S.; Shi, L.; Feng, X. Yarn-ball-shaped CNF/ MWCNT Microspheres Intercalating $Ti_3C_2T_x$ MXene for Electromagnetic Interference Shielding Films, *Carbohydr. Polym.* **2021**, 254, 117325.
7. Miao, M.; Liu, R.; Thaiboonrod, S.; Shi, L.; Cao, S.; Zhang, J.; Fang, J.; Feng, X. Silver Nanowires Intercalating $Ti_3C_2T_x$ MXene Composite Films with Excellent Flexibility for Electromagnetic Interference Shielding. *J. Mater. Chem. C* **2020**, 8, 3120.
8. Bao, S.; Zhang, M.; Jiang, Z.; Xie, Z.; Zheng, L. Advances in Microwave Absorbing Materials with Broad-bandwidth Response. *Nano Res*. **2023**, 16, 11054-11083.
9. Luckham, P. F.; Rossi, S. The Colloidal and Rheological Properties of Bentonite Suspensions. *Adv. Colloid Interface Sci*. **1999**, 82, 43-92.
10. Wu, Q.; Sjåstad, A. O.; Vistad, Ø. B.; Roots, Jr. K. D.; Pedersen, J. S.; Norby, P. Characterization of Exfoliated Layered Double Hydroxide (LDH, Mg/Al =3) Nanosheets at High Concentrations in Formamide. *J. Mater. Chem*. **2007**, 17, 965-971.
11. Maleski, K.; Mochalin, V. N.; Gogotsi, Y.; Dispersions of Two-Dimensional Titanium Carbide MXene in Organic Solvents. *Chem. Mater*. **2017**, 29, 1632-1640.
12. Shahzad, F.; Alhabeb, M.; Hatter, C. B.; Anasori, B.; Hong, S. M.; Koo, C.M.; Gogotsi, Y. Electro-magnetic Interference Shielding with 2D Transition Metal Carbides (MXenes). *Science* **2016**, 253, 1137-1140.
13. Sun, R.; Zhang, H. B.; Liu, J.; Xie, X.; Yang, R.; Li, Y.; Hong, S.; Yu, Z. Z. Highly Conductive Transition Metal Carbide/Carbonitride (MXene)@ Polystyrene Nanocomposites Fabricated by Electrostatic Assembly for Highly Efficient Electromagnetic Interference Shielding. *Adv. Funct. Mater*. **2017**, 27, 1702807.
14. Liu, J.; Zhang, H. B.; Sun, R.; Liu, Y.; Liu, Z.; Zhou, A.; Yu, Z. Z. Hydrophobic, Flexible, and Lightweight MXene Foams for High-Performance Electromagnetic-interference Shielding. *Adv. Mater*. **2017**, 29, 1702367.
15. Naguib, M.; Kurtoglu, M.; Presser, V.; Lu, J.; Niu, J.; Heon, M.; Hultman, L.; Gogotsi, Y.; Barsoum, M. W. Two-dimensional Nanocrystals Produced by Exfoliation of Ti_3AlC_2. *Adv. Mater*. **2011**, 23, 4248-4253.
16. Mani, V.; Chen, S.-M.; Lou, B.-S. Three- dimensional Graphene Oxide-Carbon Nanotubes and Graphene-Carbon Nanotubes Hybrids. *Int. J. Electrochem. Sci*. **2013**, 8, 11641-11660.
17. Liu, Y.; Li, J.; Ge, X.; Yi, S.; Wang, H.; Liu, Y.; Luo, J. Macroscale Superlubricity Achieved on the Hydrophobic Graphene Coating with Glycerol. *ACS Appl. Mater. Interfaces* **2020**, 12, 18859-18869.
18. Sun, X.; Sun, H.; Li, H.; Peng, H. Developing Polymer Composite Materials: Carbon Nanotubes or Graphene. *Adv. Mater*. **2013**, 25, 5153-5176.

19. Liang, J.; Wang, Y.; Huang, Y.; Ma, Y.; Liu, Z.; Cai, J.; Zhang, C.; Gao, H.; Chen, Y. Electromagnetic Interference Shielding of Graphene/Epoxy Composites. *Carbon* **2009**, 47, 922-925.
20. Oliveira, F. M.; Luxa, J.; Bouša, D.; Sofer, Z.; Gusmäo, R. Electromagnetic Interference Shielding by Reduced Graphene Oxide Foils. *ACS Appl. Nano Mater*. **2022**, 5, 6792-6800.
21. Jovanović, S.; Huskić, M.; Kepić, D.; Yasir, M.; Haddadi, K. A Review on Graphene and Graphene Composites for Application in Electromagnetic Shielding. *Graphene 2D Mater*. **2023**, 8, 59-80.
22. Shen, B.; Li, Y.; Yi, D.; Zhai, W.; Wei, X.; Zheng, W. Microcellular Graphene Foam for Improved Broadband Electromagnetic Interference Shielding. *Carbon* **2016**, 102, 154-160.
23. Shi, H.; Zhang, C.J.; Lu, P.; Dong, Y.; Wen, P.; Wu, Z.-S. Conducting and Lithiophilic MXene/ Graphene Framework for High-Capacity Dendrite-free lithium-metal Anodes. *ACS Nano* **2019**, 13, 14308-14318.
24. Zhou, Y.; Maleski, K.; Anasori, B.; Thostenson, J. O.; Pang, Y.; Feng, Y.; Zeng, K.; Parker, C. B.; Zauscher, S.; Gogotsi, Y.; Glass, J. T.; Cao, C. $Ti_3C_2T_x$ MXene-reduced Graphene Oxide Composite Electrodes for Stretchable Supercapacitors. *ACS Nano* **2020**, 14, 3576-3586.
25. Lee, S. H.; Eom, W.; Shin, H.; Ambade, R. B.; Bang, J. H.; Kim, H. W.; Han, T. H. Room-temperature, Highly Durable $Ti_3C_2T_x$ MXene/Graphene Hybrid Fibers for NH_3 Gas Sensing. *ACS Appl. Mater. Interfaces* **2020**, 12, 10434-10442.
26. Zhao, S.; Zhang, H.-B.; Luo, J.-Q.; Wang, Q.-W.; Xu, B.; Hong, S.; Yu, Z.-Z. Highly Electrically Conductive Three-dimensional $Ti_3C_2T_x$ MXene/ Reduced Graphene Oxide Hybrid Aerogels with Excellent Electromagnetic Interference Shielding Performances. *ACS Nano* **2018**, 12, 11193-11202.
27. Liu, J.; Liu, Z.; Zhang, H.-B.; Chen, W.; Zhao, Z.; Wang, Q.-W.; Yu, Z.-Z. Ultrastrong and Highly Conductive MXene-based Films for High-Perfor-mance Electromagnetic Interference Shielding. *Adv. Electron. Mater*. **2020**, 6, 1901094.
28. Zhang, Y.; Gao, Q.; Zhang, S.; Fan, X.; Qin, J.; Shi, X.; Zhang, G. rGO/MXene Sandwich-Structured Film at Spunlace Non-woven Fabric Substrate: Application to EMI Shielding and Electrical Heating. *J. Colloid Interface Sci*. **2022**, 614, 194-204.
29. Chen, Z.; Asif, M.; Wang, R.; Li, Y.; Zeng, X.; Yao, W.; Sun, Y.; Liao, K. Recent Trends in Synthesis and Applications of Porous MXene Assemblies: A Topical Review. *Chem. Rec*. **2022**, 22, e20210026.
30. Song, P.; Qiu, H.; Wang, L.; Liu, X.; Zhang, Y.; Zhang, J.L.; Kong, J.; Gu, J. W. Honeycomb Structural rGO-MXene/Epoxy Nanocomposites for Superior Electromagnetic Interference Shielding Performance. *Sustain. Mater. Technol*. **2020**, 24, 200153.
31. Ren, F.; Zhu, G. M.; Xie, J. Q.; Wang, K.; Cui, X. P. Cyanate Ester Filled with Graphene Nanosheets and Multi-walled Carbon Nanotubes as a Microwave Absorber. *J. Polym. Res*. **2015**, 22, 89.
32. Meng, F. B.; Wang, H. G.; Huang, F.; Guo, Y. T.; Wang, Z. Y.; Hui, D.; Zhou, Z. Graphene-Based Microwave Absorbing Composites: A Review and Prospective. *Compos. Pt. B-Eng*. **2018**, 137, 260-277.
33. Wei, Y.; Zhang, P.; Soomro, R. A.; Zhu, Q.; Xu, B. Advances in the Synthesis of 2D MXenes. *Adv. Mater*. **2021**, 33, 2103148.
34. Hummers Jr., W. S.; Offeman, R. E. Preparation of Graphitic Oxide, *J. Am. Chem. Soc*. **1958**, 80, 1339.
35. Liu, W.; Speranza, G. Tuning the Oxygen Content of Reduced Graphene Oxide and Effects on Its Properties. *ACS Omega* **2021**, 6, 6195-6205.
36. Wu, X.; Han, B.; Zhang, H. B.; Xie, X.; Tu, T.; Zhang, Y.; Yu, Z. Z. Compressible, Durable and Conductive Polydimethylsiloxane-coated MXene Foams for High-Performance Electromagnetic Interference Shielding. *Chem. Eng. J.* **2020**, 381, 122622.
37. Manobalan, S.; Suryasarathi, B.; Sumangala, T. P. Effect of Thickness on the EMI Shielding Effectiveness of Epoxy Composites with Cobalt Ferrite and Graphene. *Mater. Today: Proc*. **2023**, 90, 128-132.
38. Gudarzi, M. M. Colloidal Stability of Graphene Oxide: Aggregation in Two Dimensions. *Langmuir* **2016**, 32, 5058-5068.
39. Deville, S.; Saiz, E.; Nalla, R.K.; Tomsia, A. P. Freezing as a Path to Build Complex Composites. *Science* **2006**, 311, 515-518.
40. Plata-Gryl, M.; Castro-Munoz, R.; Boczkaj, G. Chemically Reduced Graphene Oxide Based Aerogels-Insight on the Surface and Textural Functionalities Dependent on Handling the Synthesis Factors. *Colloid Surface A* **2023**, 675, 132005.
41. Chen, W.; Yan, L. In Situ Self-Assembly of Mild Chemical Reduction Graphene for Three- Dimensional Architectures. *Nanoscale* **2011**, 3, 3132-3137.
42. Xu, Z.; Zhang, Y.; Li, P.; Cao, C. Strong, Conductive, Lightweight, Neat Graphene Aerogel Fibers with Aligned Pores. *ACS Nano* **2012**, 6, 7103-7113.
43. García-Bordejé, E.; Victor-Román, S.; Sanahuja-Parejo, O.; Benito, A. M.; Maser, W. K. Control of the Microstructure and Surface Chemistry of Graphene Aerogels via pH and Time Manipulation by a Hydrothermal Method. *Nanoscale* **2018**, 10, 3526.
44. Gao, C.; Dong, Z.; Hao, X.; Guo, S. Preparation of Reduced Graphene Oxide Aerogel and Its Adsorption for Pb(II). *ACS Omega* **2020**, 5, 9903-9911.
45. Yuan, X.; Wei, Y.; Chen, S.; Wang, P.; Liu, L. Bio-based Graphene/ Sodium Alginate Aerogels for Strain Sensors. *RSC Adv*. **2016**, 6, 64056-64064.
46. Liu, J.; Yu, M.-Y.; Yu, Z.-Z.; Nicolosi, V. Design and Advanced Manufacturing of Electro-magnetic Interference Shielding Materials. *Mater. Today* **2023**, 66, 245-272.
47. Li, C.-B.; Li, Y.-J.; Zhao, Q.; Luo, Y.; Yang, G.-Y.; Hu, Y.; Jiang, J.-J. Electromagnetic Interference Shielding of Graphene Aerogel with Layered Microstructure Fabricated via Mechanical Compression. *ACS Appl. Mater. Interfaces* **2020**, 12, 30686-30694.
48. Cheng, Z.; Wang, R.; Wang, Y.; Cao, Y.; Shen, Y.; Huang, Y.; Chen, Y. Recent Advances in Graphene Aerogels as Absorption-dominated Electromagnetic Interference Shielding Materials. *Carbon* **2023**, 205, 112-137.